Geophysical Research Letters

RESEARCH LETTER
10.1029/2023GL106632

Transient Offset in ^{14}C After the Carrington Event Recorded by Polar Tree Rings

Joonas Uusitalo[1,2], Kseniia Golubenko[3], Laura Arppe[1], Nicolas Brehm[4], Thomas Hackman[2], Hisashi Hayakawa[5,6,7,8], Samuli Helama[9], Kenichiro Mizohata[2], Fusa Miyake[5], Harri Mäkinen[10], Pekka Nöjd[10], Eija Tanskanen[11], Fuyuki Tokanai[12], Eugene Rozanov[13], Lukas Wacker[4], Ilya Usoskin[3,11], and Markku Oinonen[1]

[1]Finnish Museum of Natural History, University of Helsinki, Helsinki, Finland, [2]Department of Physics, University of Helsinki, Helsinki, Finland, [3]Space Physics and Astronomy Research Unit, University of Oulu, Oulu, Finland, [4]Laboratory of Ion Beam Physics, ETHZ, Zurich, Switzerland, [5]Institute for Space-Earth Environmental Research, Nagoya University, Nagoya, Japan, [6]Institute for Advanced Research, Nagoya University, Nagoya, Japan, [7]Science and Technology Facilities Council, RAL Space, Rutherford Appleton Laboratory, Didcot, UK, [8]Nishina Centre, Riken, Wako, Japan, [9]Natural Resources Institute Finland, Rovaniemi, Finland, [10]Natural Resources Institute Finland, Helsinki, Finland, [11]Sodankylä Geophysical Observatory, Sodankylä, Finland, [12]Faculty of Science, Yamagata University, Yamagata, Japan, [13]Physical-Meteorological Observatory Davos/World Radiation Center (PMOD/WRC), Davos, Switzerland

Key Points:

- A transient offset in ^{14}C from high-latitude Finnish Lapland tree rings was observed between years 1861 and 1863
- The Carrington event and the stratosphere-troposphere dynamics are discussed as potential explanations for the disparity
- The discovery underscores the importance of transient offsets, high-latitude tree rings in spotting anomalous solar/geomagnetic phenomena

Supporting Information:

Supporting Information may be found in the online version of this article.

Correspondence to:

J. Uusitalo,
joonas.uusitalo@helsinki.fi

Citation:

Uusitalo, J., Golubenko, K., Arppe, L., Brehm, N., Hackman, T., Hayakawa, H., et al. (2024). Transient offset in ^{14}C after the Carrington event recorded by polar tree rings. *Geophysical Research Letters*, *51*, e2023GL106632. https://doi.org/10.1029/2023GL106632

Received 1 OCT 2023
Accepted 22 FEB 2024

Abstract

The Carrington event of 1859 has been the strongest solar flare in the observational history. It plays a crucial role in shedding light on the frequency and impacts of the past and future Solar Energetic Particle (SEP) events on human societies. We address the impact of the Carrington event by measuring tree-ring ^{14}C with multiple replications from high-latitude locations around the event and by comparing them with mid-latitude measurements. A transient offset in ^{14}C following the event is observed with high statistical significance. Our state-of-the-art ^{14}C production and transport model does not reproduce the observational finding, suggesting features beyond present understanding. Particularly, our observation would require partially fast transport of ^{14}C between the stratosphere and troposphere at high latitudes. The observation is consistent with the previous findings with the SEP events of 774 and 993 CE for which faster integration of ^{14}C into tree rings is observed at high latitudes.

Plain Language Summary

Strong Earth-directed solar eruptions can cause ^{14}C concentration spikes in the atmosphere. Large enough events may leave a signal in the annually grown tree-rings as they capture the isotopic carbon fingerprint through photosynthesis. Such rapid ^{14}C increases have been detected, for instance, starting in years 774 and 993 CE. However, no increase has been observed following the Carrington event of 1859, despite it being the largest solar eruption of the modern era. Notably, all prior ^{14}C measurements covering the Carrington event come from mid-latitude trees. To achieve a broader geographical coverage, we have measured the event from several high-latitude locations. After comparing the high- and mid-latitude measurements, we have found a statistically significant difference lasting for several years post-Carrington. To better understand the difference, we have adopted a ^{14}C production and atmospheric transport model capable of simulating regional differences. Despite the improved model, we found it unable to reproduce the observational results, which suggests features beyond current understanding. Ultimately, the observation emphasizes the role of subtle ^{14}C differences in tree-ring ^{14}C studies, potentially opening new ways to study past solar phenomena and atmospheric dynamics.

1. Introduction

The assumption of geographically coherent atmospheric ^{14}C concentrations forms the basis for the radiocarbon dating method. Although this assumption is considered generally true, there is an ongoing discussion regarding the potential existence of zonal gradients or regional offsets in the measured concentrations. For example, the Northern/Southern Hemisphere ^{14}C offset is well known (Hogg et al., 2002; McCormac et al., 1998). In addition, examples of possible intra-hemispheric offsets have been reported in the past (Stuiver et al., 1998a) as well as more recently (Pearson et al., 2020). Such effects are hypothesized to reflect the changes in the long-term atmospheric or oceanic circulation patterns or be linked to latitude effects due to different growing period conditions (Kromer et al., 2001). A common challenge in studying regional offsets is that the observed differences are often at the level of the measurement uncertainties (Bayliss et al., 2020).

Table 1
List of Tree-Ring ^{14}C Datasets Used for the Present Study

Site	Region	Location	Source	Time interval
Washington, USA	mid-lat.	47°46′N 124°06′W	(Stuiver et al., 1998a)	1854–1870
Mapledurham, UK	mid-lat.	51°30′N 2°4′W	(Scifo et al., 2019)	1855–1866
Sydenham House, UK	mid-lat.	50°38′N 4°13′W	(Brehm et al., 2021)	1854–1870
Inari, Finland	high-lat.	69°30′N 27°47′E	This work	1854–1870
Värriö, Finland	high-lat.	67°44′N 29°38′E	This work	1854–1870
Hetta, Finland	high-lat.	68°18′N 23°28′E	This work	1854–1870

In addition to such long-term and large-scale phenomena, attention has recently been given to rapid and anomalous ^{14}C events discovered by Miyake et al. (2012, 2013). The initial finding sparked considerable interest, leading to additional discoveries of rapid ^{14}C increases, all found through annually resolved tree-ring measurements (e.g., Bard et al., 2023; Brehm et al., 2022; Miyake et al., 2017, 2021; O'Hare et al., 2019; Paleari et al., 2022; Park et al., 2017; Terrasi et al., 2020). These events are short production increases in ^{14}C caused by extreme solar energetic particle (SEP) events (Cliver et al., 2022; Usoskin, 2023; Usoskin et al., 2013). The results have initiated discussions of possible latitudinal differences in ^{14}C atmospheric concentrations. For example, Uusitalo et al. (2018) found that the intensity of the 774 CE event measured at high-latitude Northern locations (henceforth denoted as Northern Hemisphere 1, NH1) was significantly higher than that measured at lower latitudes. Furthermore, a signal increase already in 774 CE was demonstrated by intra-annual tree-ring measurements. Similar latitude-related differences were also observed recently for the 993 CE ^{14}C anomaly (Miyake et al., 2022). These changes were suggested to result from the atmospheric ^{14}C production limited to the polar stratosphere and the stratosphere-troposphere dynamics. Recently, Zhang et al. (2022) proposed that the statistical significance of the latitudinal gradient of the ^{14}C signal may disappear with a larger number of sites analyzed. In their analysis, they also observed distinct patterns in the peak shapes of the ^{14}C anomaly event across different locations, with some exhibiting sharp increases, while others demonstrated more gradual increases over several years. Such peak shape differences probably emphasize the role of the varying stratosphere-troposphere dynamics in shaping the observed event.

However, previous studies were based on simplified box models of the carbon cycle (e.g., Büntgen et al., 2018; Güttler et al., 2015; Oeschger et al., 1975) which by design can catch neither the latitudinal/regional differences nor precise intra-annual timescales. Moreover, none of the previous studies have detected signals in cosmogenic nuclides data around the Carrington flare, the greatest solar flare observed in the last two centuries (e.g., Cliver & Dietrich, 2013; Curto et al., 2016; Hayakawa et al., 2023).

Here, we further advance studies on the regional patterns of the atmospheric ^{14}C content by applying precise measurements and a novel direct modeling of the radiocarbon atmospheric production and transport. Particularly, we study high-latitude tree-ring ^{14}C intensities across the Carrington event. As a main result, we report on a statistically separable transient offset of ^{14}C measured in high-latitude tree rings as compared to lower-latitude locations. This offset lasted for several years after the Carrington flare of 1859. We discuss the potential origin of the disparity by considering possible solar and geomagnetic effects as well as the complex atmospheric dynamics. The finding opens new possibilities in studies of the fine structure of the past ^{14}C records and solar and geomagnetic phenomena within the present era of increasing numbers of annually resolved measurements.

2. Materials and Methods

2.1. Measurements and Other Data

The sample set contains new measurements of $\Delta^{14}C$ in tree-ring material of three individual trees (*Pinus sylvestris*) from three distinct locations in northern Finland (Inari, Värriö, and Hetta – see Table 1 and Figure S1 in Supporting Information S1). Dendrochronological analyses and extraction of annually resolved tree-ring samples were performed by the Natural Resources Institute Finland. The samples were processed to cellulose and decay-corrected $\Delta^{14}C$ values were measured by the Laboratory of Chronology/University of Helsinki (Uusitalo et al., 2022), Yamagata University (Takeyama et al., 2023) and IonBeam Lab/ETH Zurich

(Sookdeo et al., 2020; Wacker et al., 2010) as specified in Supplementary Table S1. The sample set comprises a total of 116 measurements spanning the years 1854–1870. We hereby discuss these as high-latitude data.

In addition, the analyzed data set includes data (see Table 1) from Washington (USA), Mapledurham (UK) and Sydenham House (UK), all spanning through the Carrington event period. We define these as mid-latitude data. Furthermore, for comparing the statistical significance of annual tree-ring ^{14}C differences between high- and mid-latitude measurements, we also used data from Friedrich et al. (2019), which covers the period 382–460 CE.

2.2. Mean Calculation and Statistical Comparisons

The yearly mean ^{14}C values and their uncertainties for both the high- and mid-latitude zones were calculated through Monte Carlo simulation. Specifically, for each year, a mean value is calculated by simulating new values based on the errors of the individual ^{14}C measurements and then calculating the average of those simulated values. The previous step is repeated 100,000 times for each year. The final mean estimate and the uncertainty for each year is calculated by taking the average and standard deviation of the simulated values. The described Monte Carlo method propagates the measurement uncertainties, with the mean being derived from the observed dispersion. We note that calculated uncertainty estimates do not account for the potential over-dispersion, meaning that the final error is derived from the measurement uncertainties only. This is a well-recognized challenge facing all tree-ring-based ^{14}C measurements (Heaton et al., 2020; Scott et al., 2023). Our aim with the numerous replications spanning different locations, trees and measurement protocols, has been to shed light on this potential variability beyond measurement uncertainties. To further mitigate the potential effects of over-dispersion, we calculated centered 3-year moving averages for both the high- and mid-latitude data sets. The moving average gives robust estimates for the central tendencies of both the high- and mid-latitude data. The centered 3-year moving averages are calculated using a similar Monte Carlo simulation approach as for the annual means. In this case, measurements within a 3-year window are combined (e.g., for the year 1855, values from 1854 to 1856 are used). The procedure is then carried out for years 1855–1869. Finally, We assess the potential presence of outliers in the annual high latitude data with the Grubbs test (Grubbs, 1969). For statistical comparisons between data sets, we use the Z-test to be consistent with the past International Radiocarbon Intercomparison studies (Scott et al., 2018) and measurements of Friedrich et al. (2019).

2.3. Modeling of ^{14}C Production and Transport

For this study, the production of ^{14}C was computed using the CRAC (Cosmic-Ray Atmospheric Cascade) model (Poluianov et al., 2016), which is the most recent and precise model of cosmogenic isotope production. Because we do not know the real energy spectrum of the Carrington event we use a hard spectrum of the second strongest and best studied SEP event of 20-Jan-2005 (GLE #69 – see http://gle.oulu.fi) computed by Koldobskiy et al. (2021). The corresponding isotope production rates were used as input parameters for the Chemical Climate Model (CCM) SOCOL-AERv2 (Chemistry-Climate Model SOlar Climate Ozone Links with AERosol module Version 2) (Feinberg et al., 2019). This model version consists of the general circulation model MA-ECHAM5 (Hommel et al., 2011) and the atmospheric chemistry module MEZON (Egorova et al., 2003), which interact with each other every two modeling hours. The CCM SOCOL-AERv2 was extended with the Carbon 14 module, as was done previously for Beryllium 7 (Golubenko et al., 2021). The exchange between different carbon reservoirs is represented through differential fluxes, and the exchange coefficients were adopted from box models (Fairhall & Young, 1985; Güttler et al., 2015; Oeschger et al., 1975), namely 7.3 and 1.8 years for the ocean and land, respectively. Carbon sinks are implemented through decay times and are dependent on the surface type (ocean or land). Depending on latitude, ^{14}C sinks into the land in different seasons: throughout the year in equatorial latitudes (0–30°), from April to October in middle latitudes (30–55°), from May to September in pre-polar latitudes (55–65°), and there is no sinking in polar latitudes (65–90°). The sinking into the ocean occurs throughout the year in all latitudes. More details on the model based on (Fairhall & Young, 1985; Güttler et al., 2015; Oeschger et al., 1975; Stenke et al., 2013) can be found in the Text S1 in Supporting Information S1.

3. Results

Data of the annually averaged $\Delta^{14}C$ in high- and mid-latitude zones are depicted in Figure 1. As seen in Figure 1a, there is a systematic and statistically significant difference between the high- and mid-latitude measurements from

10.1029/2023GL106632

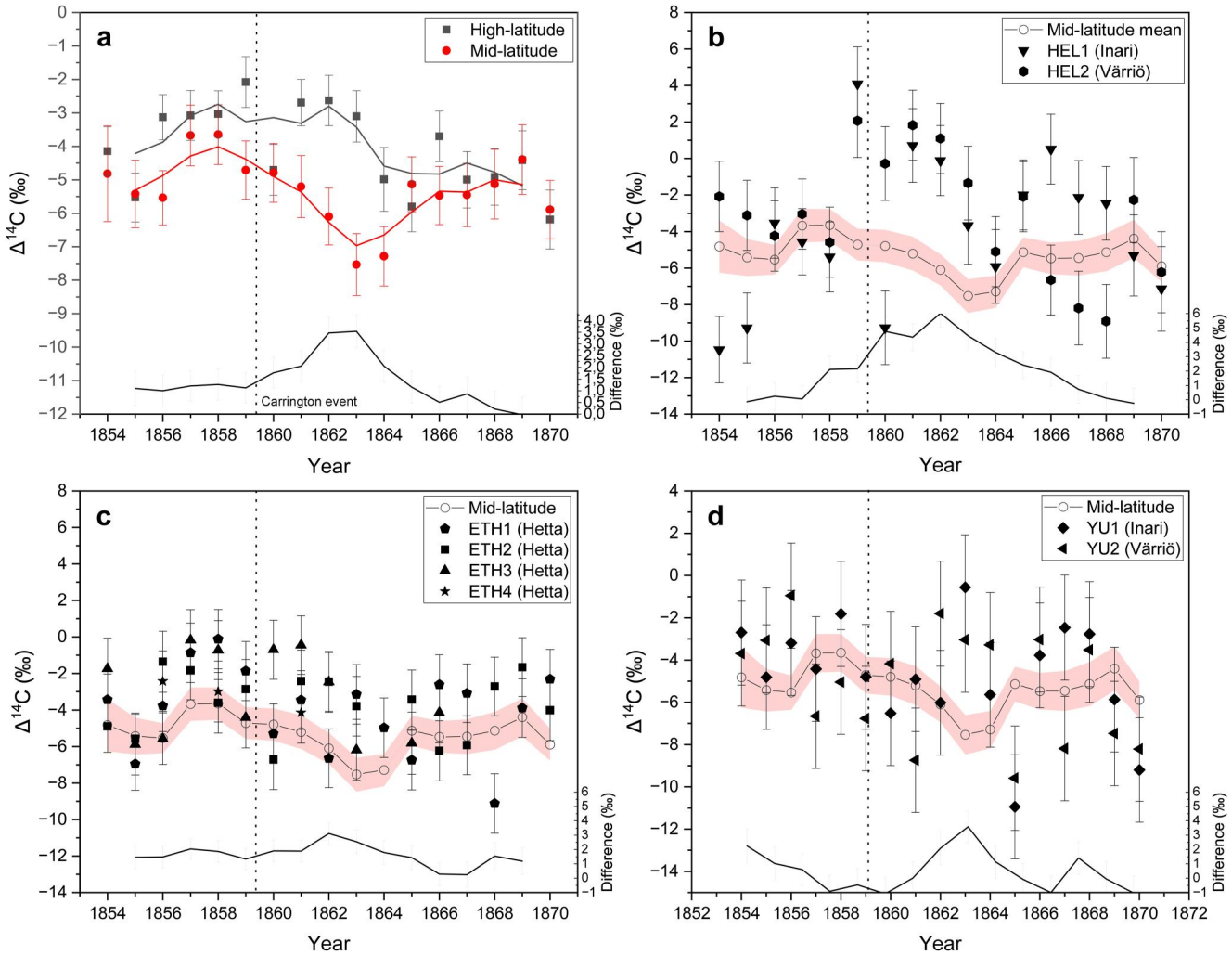

Figure 1. Panel (a) shows the $\Delta^{14}C$ data measured around the Carrington event, denoted by the vertical dashed line. The black squares show the mean of the high latitude data as measured from three different trees (see Table 1 and Methods). Each annual point includes 5–8 measurements (see Table S1). The red circles depict the mean annual values for the mid-latitude dataset. Each point includes three (for years 1855–1866) or two measurements. Uncertainties correspond to one standard error. The black and the red lines denote the 3-year moving averages of the high- and mid-latitude datasets, respectively. The bottom part of each panel shows the difference between the 3-year moving average curves, with the y-scale for this section on the right side. Panels (b)–(d) show the individual measurements of the high-latitude data versus mid-latitude average from different trees and laboratories, as detailed in Table 1 and Supplementary Table S1. For clarity, all data points are aligned with full years, though the actual growing periods are approximated to mid-year.

1861 to – 1863, such that the ^{14}C contents measured in tree rings from northern Finland are enhanced by a few permil compared to those in the mid-latitude region. Figures 1b and 1d show all the individual measurements partitioned by the different measurement laboratories. The individual measurements display noticeable variance, attributable to measurement uncertainties, but possibly also to factors such as varying locations, tree species, and laboratory procedures. All the panels show increased values compared to the mid-latitude means around the years 1861–1863, with the tree from Hetta (panel d) showing somewhat increased values already before. The general central tendency of the difference between high- and mid-latitude data is clearer when comparing the 3-year moving averages as indicated by the bottom curve in Figure 1a. The difference has an offset of ca. 1 permil, increases to 3.5 permil ca. 1862 and then gradually decreases, forming a distinct peak shape. The offset is also present in each of the individual laboratory comparisons, as illustrated in the bottom parts of Figures 1b and 1d: HEL, ETH and YU measurements reach peak offsets of 6.0, 3.1 and 3.6 permil, respectively, around years 1862–1863.

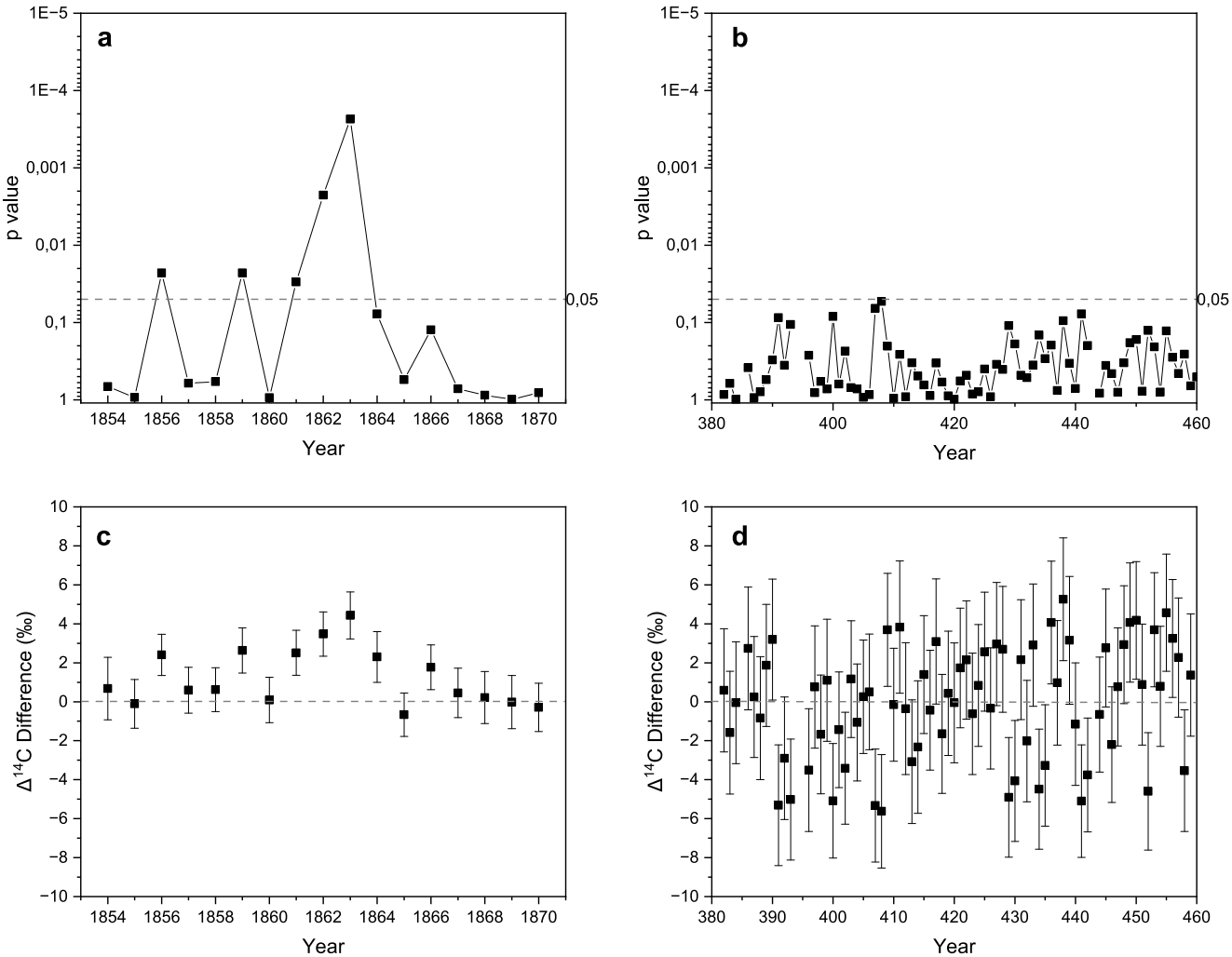

Figure 2. Comparison of the high-versus mid-latitude $\Delta^{14}C$ differences across two different time periods. Panels (a) and (b) depict the statistical significance (in terms of *p*-value) of the differences in $\Delta^{14}C$ for two time periods: (a) around the Carrington flare, and (b) for the period of 382–460 CE (see Methods). The dashed horizontal lines mark the 0.05 significance level. The *y*-axis is inverted and logarithmic. Panels (c) and (d) present the absolute $\Delta^{14}C$ differences for the same time periods as those depicted in panels (a) and (b), with the dashed horizontal line marking the baseline.

The statistical significance of the difference between high- and mid-latitude annual data at the time around the Carrington flare is further explored in Figure 2a. The difference appears systematic and highly significant (*p*-value is below 0.01) for the years 1862 and 1863, and significant ($p < 0.05$) for the year 1861. For all other analyzed years, the difference is insignificant ($p > 0.05$) except for years 1856 and 1859 when the difference is significant ($p \approx 0.02$). With regards to p-values, it is important to note that they are calculated based on the annual mean values and their standard errors, which are propagated from the individual measurement errors. Although this is a common practice, the final uncertainty may not fully represent the underlying distribution, thereby possibly affecting the individual p-value comparisons. Hence, it is better to look at the overall behavior, rather than individual points. The fact that the p-value is low on multiple adjacent points strengthens the interpretation that the difference is real and not a statistical anomaly. Furthermore, based on the two-sided Grubbs test (see Methods), the high-latitude measurements show internal consistency with no significant outliers at the $p = 0.05$ level, apart from years 1854 and 1864. For 1864, the apparent outlier results from low variance and fewer measurements, with four out of five falling within 1 permil. The measurement identified as an outlier is 1.7 permil above that year's average, a normal fluctuation within single measurements. In 1854, an outlier is detected as 6.3 permil below the average. However, we retained this outlier in the analysis as it did not occur during key years and does not affect the interpretation of the results.

Finally, although the high-latitude measurements are consistent as a group, there are occasional differences in pair-wise comparisons between laboratories. Furthermore, the HEL measurements display a more pronounced offset. To assess whether the offset is influenced by extremities, we have performed sensitivity analyses where, for each year in the high-latitude data, the value furthest from the mean is excluded, and as a separate test where both extremes (min-max) are excluded. We found that the ^{14}C difference remained essentially unchanged (see Figure S2 in Supporting Information S1). Furthermore, the transient offset persists even if the HEL measurements are excluded altogether from the comparison (see Figure S3 in Supporting Information S1). In addition, we have calculated the 3-year moving median of the high-latitude data and its difference from the mid-latitude data. As the median is the value in the middle of the data set, it is not sensitive to extreme values. The resulting graph (see Figure S2 in Supporting Information S1) of the difference is essentially the same as the one calculated using the moving means shown in Figure 1a. This consistency between the two methods reinforces our observation that the transient offset is robust against the influence of individual values.

Although the difference is statistically significant, it may potentially arise from a general bias between the high- and mid-latitude ^{14}C concentrations or incorrectly estimated natural variability inherent to each latitude zone. To test this, we performed a similar comparison between high- and mid-latitude ^{14}C data (Friedrich et al., 2019) spanning years 382–460 CE (Figure 2b). As seen, none of the 79 points appears significant at $p < 0.05$ level suggesting that annual differences as significant as those observed after the Carrington flare are not common among measurements with similar latitude profiles. However, to our knowledge, the annual data is not comprised of as many and as varied measurements as in our comparison, leading to larger uncertainties in estimation of the mean. This is further demonstrated in Figures 2c and 2d, which show the absolute difference for the Carrington and 382–460 periods, respectively. From the comparison, the latter clearly exhibits more variance. Although the data shows occasional diversions being as large or even larger than during the Carrington period, they appear to be more random in nature, as demonstrated by their scatter on both sides of the baseline. On the other hand, the Carrington era difference shows remarkable stability, with most values residing on the baseline, except for the years 1861–1864. In summary, the data of Friedrich et al. does not show evidence for excursions like what is observed around the Carrington event. However, the existence of such transient differences cannot be completely ruled out, as the annual sample size of Friedrich et al.'s measurements may not be sufficiently large to provide the necessary statistical power.

4. Discussion

We show that a statistically significant difference exists between ^{14}C abundances at high- and mid-latitude following the Carrington flare. The found divergence is a short-term (several years) transient phenomenon and appears distinct from more persistent offsets due to geographical growth-period differences (Stuiver & Braziunas, 1998). Independent measurements of the samples by multiple laboratories make the results robust against possible biases related to statistics or measurement processes, an issue typically affecting annual ^{14}C comparisons. Below we discuss the potential origin of the observed difference by considering geomagnetic effects, the Carrington event, atmospheric circulations and the solar cycle.

The years around the Carrington event - and during the solar cycle 10 - were geomagnetically unusually active. The Helsinki magnetic observatory measured enhanced numbers of geomagnetic storm days around 1860–1866 and auroral intensities were similarly elevated (Nevanlinna & Kataja, 1993). Moreover, the wandering of the north magnetic pole (https://www.ngdc.noaa.gov/geomag/data/poles/NP.xy) changed its direction around 1860 and similar phenomena occurred in 1730 (Kovalyov, 2019). The increased and dynamic activity is also demonstrated by geomagnetic jerks observed around those years (e.g., 1861/1870; 1730/1741) (Alexandrescu et al., 1997; Korte et al., 2009). Interestingly, these geomagnetic jerks essentially coincide with the historically observed geomagnetic storms induced by the Carrington flare and that of the year 1730 (Hayakawa et al., 2018). These simultaneous phenomena may indicate a solar-terrestrial connection within the dynamic development of the geomagnetic field.

However, the Carrington event itself has been considered one of the most significant geomagnetic storms. Whereas the model discussed here assumes a constant eccentric-dipole geomagnetic field during the period in question, the Carrington flare induced an extreme geomagnetic disturbance of the Disturbance H variations of −917 to −989 nT according to the Colaba magnetometer (Hayakawa et al., 2022). Considering the Colaba magnetogram data for the September 1–2 storm, the decrease in the horizontal geomagnetic field seems small.

Averaging over the full year, the decrease of the geomagnetic field strength was still less than 1% of the full horizontal field strength. Moreover, the observed latitudinal gradient is difficult to conceive due to such a global geomagnetic field disturbance. Thus, we consider the contemporary GM field change to be of minor importance in our observation.

Although no definite quantitative explanations can be given to the observed excess of high-latitude ^{14}C atmospheric abundances over the mid-latitude ones in the early 1860s, some qualitative understanding can be proposed. Given the concurrent timing, the first idea would be that the observed ^{14}C polar enhancement was caused by a solar energetic particle (SEP) event associated with the Carrington flare, since ^{14}C production by SEPs mostly occurs at higher latitudes (Golubenko et al., 2022). To check this idea, we utilized a CCM SOCOL (see Methods) to determine whether the observed divergence could be explained in the model's framework. However, according to the model simulations made assuming a constant geomagnetic dipole field and the hard energy spectrum of the strong SEP event of 20-Jan-2005 (GLE #69), we were unable to reproduce the observation of enhanced tropospheric ^{14}C content at high latitudes (see Figure S4 and Text S1 in Supporting Information S1). Thus, the statistically significant polar enhancement needs further explanation beyond the used model assumptions.

This enhancement took place a few years after the Carrington flare in September 1859. The flare magnitude has been indirectly estimated as ≈X64.4 ± 7.2 (≈5×10^{32} erg of bolometric energy) from the magnitude of the geomagnetic crochet (solar-flare effect) (Cliver et al., 2022). Recent assessments have revised the magnitude estimate even upward ≈X80 (X46–X126) and ≈$(5.77 \pm 2.89) \times 10^{32}$ erg on the basis of areas of white-light flaring regions, flare duration, and brightness descriptions (Hayakawa et al., 2023). This means that the Carrington flare was more intense than the most intense solar flares in observational history. Moreover, the auroral reports indicate a precursor solar flare with significant intensity in late August 1859 (Cliver & Dietrich, 2013; Hayakawa et al., 2019). As such, the upward revision for the Carrington flare and the presence of the August flare are rather supportive for an expectation of an extreme SEP event causing $\Delta^{14}C$ enhancements in the Arctic tree rings. In addition, a total solar eclipse on 18 July 1860 allowed contemporaneous astronomers to witness the earliest coronal mass ejection in observational history (Eddy, 1974; Hayakawa et al., 2021). This probable interplanetary coronal mass ejection launched from the southwestern quadrant of the solar disk which is favorable for a geoeffective SEP event. This may have contributed to the observation, although we need to be cautious not to overinterpret the associations of the indirectly observed flares with the $\Delta^{14}C$ enhancements. Particularly, the enhancement observed in tree-rings would require mostly stratospheric ^{14}C excess to be transported to ground level for photosynthetic fixation.

According to atmospheric ozone tracking studies, the injection of stratospheric air into the troposphere occurs primarily as the stratospheric-tropospheric exchange (STE) during the spring season at latitudes between 40 and – 80°N, with 19–33% of air mass exchange taking place at latitudes above 70°N (Liang et al., 2009). The atmospheric Brewer-Dobson circulation is typically referred to in relation to the ^{14}C tree-ring studies as the main mechanism behind the global STE. Although this circulation controls the downwelling of air into the lower stratosphere, the air exchange across the tropopause occurs through smaller scale processes, such as tropopause folds near the jet streams (Rao & Kirkwood, 2005), especially at mid-latitudes. Significant STE also occurs at the high Arctic latitudes of around 70°N, often referred to as the "Arctic Front" (Dibb et al., 1992, 1994, 2003; Shapiro et al., 1987). This region is zonally close to the high-latitude region where our analyzed trees grew. Furthermore, according to a recent stratospheric ozone intrusion study with measurements from North American locations, there is a tendency for larger stratospheric contributions to the middle and upper tropospheric layers for latitudes north of 60°N compared to lower latitude zones, likely because the Arctic tropopause resides at lower altitudes compared to the more southern latitudes (Tarasick et al., 2019).

The above-described fast Arctic STE has potentially gained supporting evidence from recent studies of SEP events of 774 and 993 CE. A fast rise of ^{14}C level in high-latitude trees in Finnish Lapland (Uusitalo et al., 2018) and Yamal (Jull et al., 2014) has been observed in 774 CE. Furthermore, an early elevated signal in high-latitude trees has been observed in 993 CE (Miyake et al., 2022). Such observations cannot be understood assuming that atmospheric ^{14}C transport occurs solely through mid-latitudes, unless production occurred near ground levels at high latitudes. In fact, considering the 993 CE event, it is puzzling why there is no increase at all in the mean values of the low latitude zone (NH2) for the year 993 CE, as opposed to the more northern locations of NH1 and particularly of NH0 (Figure 4d of Miyake et al., 2022). All the above indicate fast high-latitude transport of stratospheric air to troposphere consistent with Liang et al. (2009).

Eventually, the peak maxima are reached 2–3 years after the 774 and 993 CE events. We note a similarity with our observed divergence, where the difference forms a trend that keeps increasing and peaks 3 years after the event. For all the events, the stratosphere appears injecting ^{14}C to the high-latitude troposphere for several years after the event. Thereby, we consider the possibility that the underlying mechanism for the observed divergence may share similarities to those suggested for the 774 and 993 CE events. Namely that part of the initial Arctic stratospheric/upper tropospheric ^{14}C excess transports relatively quickly to the ground level at high latitudes and gets fixated to the trees before the signal gets diluted by the greater atmospheric volumes in mid- and low-latitude regions. Only later, after a more complete stratospheric mixing, would the tropospheric concentrations be dominated by the mid- and high-latitude air injections. Meanwhile, the midlatitude ^{14}C, with larger air masses, would be dominated by changes in galactic cosmic ray (GCR) intensity caused by the Schwabe cycle (Golubenko et al., 2022), leading to decreasing concentrations. Those decreases would be countered by the Carrington event excess in the high-latitude trees thus forming the observed divergence.

Furthermore, we note that to make this hypothesis feasible, the Arctic upper atmosphere needs to be isolated long enough to allow for the ^{14}C excess to affect the troposphere for a few years before fully mixing with the larger stratosphere. Similar behavior has indeed been observed before, following the Soviet nuclear bomb tests at Novaya Zemlya (73°N) that injected huge amounts of ^{14}C into the Arctic stratosphere during 1961/1962. After the largest detonations, it took several years for the stratospheric concentrations to get well mixed, with the Arctic stratosphere demonstrating larger concentrations altitude-wise compared to the more southern regions (see Figure 33 and onwards in Telegadas, 1971). However, we note that in general, the ^{14}C bomb peak proves suboptimal as an analog for the Carrington event and the subsequent tropospheric excess, due to the diverse geographies, differing latitude zones, and varied altitude ranges associated with the numerous nuclear tests conducted by several nations during the late 1950's and early 1960's.

An alternative explanation can be related to the solar cycle. According to models (e.g., Golubenko et al., 2022; Kovaltsov et al., 2012), the global production rate of ^{14}C changes by 15–20% over a typical solar cycle, leading to 1–3‰ fluctuations in mid-latitude $\Delta^{14}C$ tree-ring data (Brehm et al., 2021; Friedrich et al., 2019; Kudsk et al., 2022). Potentially, such fluctuations may also result in short-term inhomogeneities of the order of several permille in ground-level concentrations. This would require stratospheric production gradients and rapid STE at high latitudes in a similar manner to what was hypothesized in relation to the Carrington flare. Although this is not supported by direct modeling, such a mechanism can suggestively lead to occasional asynchronicity in the solar-cycle $\Delta^{14}C$ minima and maxima observed in high- and mid-latitude records (Friedrich et al., 2019). Our high statistical precision based on multiple measurements demonstrates that it is possible to detect several-permille variations in the tree-ring $\Delta^{14}C$ signals.

As a summary, we report a robust observational result of a transient $\Delta^{14}C$ offset after the Carrington event. The offset cannot be understood in the framework of the current paradigm, as demonstrated by the modeling results. We have discussed the observation through the recent upscaled magnitude of the Carrington flare in combination with the less well-understood Arctic STE dynamics, to help explain both the offset, as well as the rapid high-latitude signals in the 774 CE and 993 CE events. We note that additional measurements from high- and mid-latitude locations are needed to be more conclusive of the exact cause. To pinpoint the exact cause, we propose replicated measurements across multiple solar cycles and further study of potential analogous events from for example, years 1052/1054, 1279, 1582, 1730 and 1770 (Brehm et al., 2021; Hattori et al., 2019; Hayakawa et al., 2017, 2018; Terrasi et al., 2020). If such transient offsets are prevalent, they could provide a novel method for studying past solar, geomagnetic and atmospheric phenomena. By improving the detection of smaller SEP events, they could help bridge the gap (Usoskin & Kovaltsov, 2021) between the very large/medium-sized events (e.g., 774 and 993 CE) and the much smaller ones observed through modern instrumental methods. An improved understanding of the statistics of extreme solar events would be valuable when assessing the potential societal risks they pose. Furthermore, they may provide important insights into the multifaceted atmospheric dynamics and STE processes free of the contaminations of the modern era with anthropogenic radionuclide and fossil carbon signals.

Data Availability Statement

The high-latitude tree-ring ^{14}C measurements and the ^{14}C production and transport modeling data are presented in Tables S1 and S2 of this article, respectively. Additionally, these datasets are available in the Zenodo repository

(Uusitalo et al., 2024). The mid-latitude tree-ring ^{14}C data for the Carrington period can be accessed from the original publications of Stuiver et al. (1998b), Scifo et al. (2019), and Brehm et al. (2021), and also from Table S1 of this article. The high- and mid-latitude tree-ring ^{14}C data for the period 382–460 CE can be accessed from Friedrich et al. (2019).

Acknowledgments

The work of Laboratory of Chronology and LUKE has been supported by the Research Council of Finland projects CARATE and QUANOMAL (251287, 251441, 288083, 288267). The work of JU has been supported by personal grants from Magnus Ehrnrooth foundation, Finnish Cultural Foundation and Emil Aaltonen foundation. JU and MO wish to thank Hanna Turunen, Anne-Maija Forss, Kari Eskola and Igor Shevchuk for sample pretreatment and isotope work, and Pietari Kienanen for AMS analyses. The measurements at the University of Helsinki and the work of TH were supported by the Research Council of Finland project SOLSTICE (decision no. 324161). IU and KG work was supported by the Research Council of Finland (Projects ESPERA no. 321882 and GERACLIS 354280). IU and HH's work benefited from the discussions in the framework of the International Space Science Institute (ISSI) team 510 "SEESUP—Solar Extreme Events: Setting Up a Paradigm". KG expresses gratitude to Dr. Timofei Sukhodolov from PMOD/WRC for their consultations and assistance in the development of the new Carbon 14 module creation based on CCM SOCOL. HH's work was financially supported in part by JSPS Grant-in-Aids JP20K22367, JP20K20918, JP20H05643, JP20K04032, JP21H01131, JP21J00106, and JP21K13957, JSPS Overseas Challenge Program for Young Researchers, and the ISEE director's leadership fund for FY2021, Young Leader Cultivation (YLC) programme of Nagoya University, Tokai Pathways to Global Excellence (Nagoya University) of the Strategic Professional Development Program for Young Researchers (MEXT), and the young researcher units for the advancement of new and undeveloped fields, Institute for Advanced Research, Nagoya University of the Program for Promoting the Enhancement of Research Universities. FM's work was supported by JSPS Grant-in-Aids JP20K20918, JP20H05643, JP20H00035, JP20H01369, and JP19H00706. ChatGPT has been used as a tool for grammar checking when preparing this manuscript.

References

Alexandrescu, M., Courtillot, V., & Le Mouël, J.-L. (1997). High-resolution secular variation of the geomagnetic field in western Europe over the last 4 centuries: Comparison and integration of historical data from Paris and London. *Journal of Geophysical Research: Solid Earth*, *102*(B9), 20245–20258. https://doi.org/10.1029/97JB01423

Bard, E., Miramont, C., Capano, M., Guibal, F., Marschal, C., Rostek, F., et al. (2023). A radiocarbon spike at 14,300 cal yr BP in subfossil trees provides the impulse response function of the global carbon cycle during the late glacial. *Philosophical Transactions. Series A, Mathematical, Physical, and Engineering Sciences*, *381*(2261). https://doi.org/10.1098/rsta.2022.0206

Bayliss, A., Marshall, P., Dee, M. W., Friedrich, M., Heaton, T. J., & Wacker, L. (2020). IntCal20 tree rings: An archaeological swot analysis. *Radiocarbon*, *62*(4), 1045–1078. https://doi.org/10.1017/RDC.2020.77

Brehm, N., Bayliss, A., Christl, M., Synal, H. A., Adolphi, F., Beer, J., et al. (2021). Eleven-year solar cycles over the last millennium revealed by radiocarbon in tree rings [Dataset]. Nature Geoscience, *14*(1), 10–15. https://doi.org/10.1038/S41561-020-00674-0

Brehm, N., Christl, M., Knowles, T. D. J., Casanova, E., Evershed, R., Adolphi, F., et al. (2022). Tree-rings reveal two strong solar proton events in 7176 and 5259 BCE. *Nature Communications*, *13*(1), 1196. https://doi.org/10.1038/s41467-022-28804-9

Büntgen, U., Wacker, L., Galvan, J., Arnold, S., Arseneault, D., Baillie, M., et al. (2018). Tree rings reveal globally coherent signature of cosmogenic radiocarbon events in 774 and 993 CE. *Nature Communications*, *9*(1), 3605. https://doi.org/10.1038/s41467-018-06036-0

Cliver, E., Schrijver, C., Shibata, K., & Usoskin, I. (2022). Extreme solar events. *Living Reviews in Solar Physics*, *19*(2), 2. https://doi.org/10.1007/s41116-022-00033-8

Cliver, E. W., & Dietrich, W. F. (2013). The 1859 space weather event revisited: Limits of extreme activity. *Journal of Space Weather and Space Climate*, *3*(26), A31. https://doi.org/10.1051/swsc/2013053

Curto, J. J., Castell, J., & Del Moral, F. (2016). SFE: Waiting for the big one. *Journal of Space Weather and Space Climate*, *6*, A23. https://doi.org/10.1051/swsc/2016018

Dibb, J. E., Meeker, L. D., Finkel, R. C., Southon, J. R., Caffee, M. W., & Barrie, L. A. (1994). Estimation of stratospheric input to the arctic troposphere: ^{7}Be and ^{10}Be in aerosols at Alert, Canada. *Journal of Geophysical Research*, *99*(D6), 12855–12864. https://doi.org/10.1029/94JD00742

Dibb, J. E., Talbot, R. W., & Gregory, G. L. (1992). Beryllium 7 and lead 210 in the western hemisphere Arctic atmosphere: Observations from three recent aircraft-based sampling programs. *Journal of Geophysical Research: Atmospheres*, *97*(D15), 16709–16715. https://doi.org/10.1029/91JD01807

Dibb, J. E., Talbot, R. W., Scheuer, E., Seid, G., DeBell, L., Lefer, B., & Ridley, B. (2003). Stratospheric influence on the northern North American free troposphere during TOPSE: 7Be as a stratospheric tracer. *Journal of Geophysical Research: Atmospheres*, *108*(D4), 11–1. https://doi.org/10.1029/2001JD001347

Eddy, J. A. (1974). A nineteenth-century coronal transient. *Astronomy and Astrophysics*, *34*, 235.

Egorova, T., Rozanov, E., Zubov, V., & Karol, I. (2003). Model for investigating ozone trends MEZON. *Izvestiya - Atmospheric and Oceanic Physics*, *39*, 277–292.

Fairhall, A. W., & Young, J. A. (1985). Historical ^{14}C measurements from the Atlantic, Pacific, and Indian oceans. *Radiocarbon*, *27*(3), 473–507.

Feinberg, A., Sukhodolov, T., Luo, B.-P., Rozanov, E., Winkel, L. E., Peter, T., & Stenke, A. (2019). Improved tropospheric and stratospheric sulfur cycle in the aerosol-chemistry-climate model SOCOL-AERv2. *Geoscientific Model Development*, *12*(9), 3863–3887. https://doi.org/10.5194/gmd-12-3863-2019

Friedrich, R., Kromer, B., Sirocko, F., Esper, J., Lindauer, S., Nievergelt, D., et al. (2019). Annual ^{14}C tree-ring data around 400 AD: Mid- and high-latitude records [Dataset]. Radiocarbon, *61*(5), 1305–1316. https://doi.org/10.1017/RDC.2019.34

Golubenko, K., Rozanov, E., Kovaltsov, G., Leppänen, A.-P., Sukhodolov, T., & Usoskin, I. (2021). Chemistry-climate model SOCOL-AERv2-BEv1 with the cosmogenic beryllium-7 isotope cycle. *Geoscientific Model Development Discussions*, *2021*, 1–24. https://doi.org/10.5194/gmd-2021-56

Golubenko, K., Rozanov, E., Kovaltsov, G., & Usoskin, I. (2022). Zonal mean distribution of cosmogenic isotope (^{7}Be, ^{10}Be, ^{14}C, and ^{36}Cl) production in stratosphere and troposphere. *Journal of Geophysical Research: Atmospheres*, *127*(16), e2022JD036726. https://doi.org/10.1029/2022JD036726

Grubbs, F. E. (1969). Procedures for detecting outlying observations in samples. *Technometrics*, *11*(1), 1–21. https://doi.org/10.1080/00401706.1969.10490657

Güttler, D., Adolphi, F., Beer, J., Bleicher, N., Boswijk, G., Christl, M., et al. (2015). Rapid increase in cosmogenic ^{14}C in AD 775 measured in New Zealand kauri trees indicates short-lived increase in ^{14}C production spanning both hemispheres. *Earth and Planetary Science Letters*, *411*, 290–297. https://doi.org/10.1016/j.epsl.2014.11.048

Hattori, K., Hayakawa, H., & Ebihara, Y. (2019). Occurrence of great magnetic storms on 6–8 march 1582. *Monthly Notices of the Royal Astronomical Society*, *487*(3), 3550–3559. https://doi.org/10.1093/mnras/stz1401

Hayakawa, H., Bechet, S., Clette, F., Hudson, H. S., Maehara, H., Namekata, K., & Notsu, Y. (2023). Magnitude estimates for the Carrington flare in 1859 September: As seen from the original records. *The Astrophysical Journal Letters*, *954*(1), L3. https://doi.org/10.3847/2041-8213/ACD853

Hayakawa, H., Ebihara, Y., Vaquero, J. M., Hattori, K., Carrasco, V. M. S., Gallego, M. d. l. C., et al. (2018). A great space weather event in February 1730. *Astronomy and Astrophysics*, *616*, A177. https://doi.org/10.1051/0004-6361/201832735

Hayakawa, H., Ebihara, Y., Willis, D. M., Toriumi, S., Iju, T., Hattori, K., et al. (2019). Temporal and spatial evolutions of a large sunspot group and great auroral storms around the Carrington event in 1859. *Space Weather*, *17*(11), 1553–1569. https://doi.org/10.1029/2019SW002269

Hayakawa, H., Iwahashi, K., Ebihara, Y., Tamazawa, H., Shibata, K., Knipp, D. J., et al. (2017). Long-lasting extreme magnetic storm activities in 1770 found in historical documents. *The Astrophysical Journal Letters*, *850*(2), L31. https://doi.org/10.3847/2041-8213/aa9661

Hayakawa, H., Lockwood, M., Owens, M. J., Sôma, M., Besser, B. P., & van Driel-Gesztelyi, L. (2021). Graphical evidence for the solar coronal structure during the Maunder minimum: Comparative study of the total eclipse drawings in 1706 and 1715. *Journal of Space Weather and Space Climate*, *11*, 1. https://doi.org/10.1051/swsc/2020035

Hayakawa, H., Nevanlinna, H., Blake, S. P., Ebihara, Y., Bhaskar, A. T., & Miyoshi, Y. (2022). Temporal variations of the three geomagnetic field components at Colaba observatory around the Carrington storm in 1859. *The Astrophysical Journal*, *928*(1), 32. https://doi.org/10.3847/1538-4357/ac2601

Heaton, T. J., Blaauw, M., Blackwell, P. G., Ramsey, C. B., Reimer, P. J., & Scott, E. M. (2020). The IntCal20 approach to radiocarbon calibration curve construction: A new methodology using Bayesian splines and errors-in-variables. *Radiocarbon*, *62*(4), 821–863. https://doi.org/10.1017/RDC.2020.46

Hogg, A. G., McCormac, F. G., Higham, T. F. G., Reimer, P. J., Baillie, M. G. L., & Palmer, J. G. (2002). High-precision radiocarbon measurements of contemporaneous tree-ring dated wood from the British Isles and New Zealand: Ad 1850–950. *Radiocarbon*, *44*(3), 633–640. https://doi.org/10.1017/S0033822200032082

Hommel, R., Timmreck, C., & Graf, H. F. (2011). The global middle-atmosphere aerosol model MAECHAM5-SAM2: Comparison with satellite and in-situ observations. *Geoscientific Model Development*, *4*(3), 809–834. https://doi.org/10.5194/gmd-4-809-2011

Jull, A. J. T., Panyushkina, I. P., Lange, T. E., Kukarskih, V. V., Myglan, V. S., Clark, K. J., et al. (2014). Excursions in the ^{14}C record at ad 774-775 in tree rings from Russia and America. *Geophysical Research Letters*, *41*(8), 3004–3010. https://doi.org/10.1002/2014GL059874

Koldobskiy, S. A., Raukunen, O., Vainio, R., Kovaltsov, G., & Usoskin, I. (2021). New reconstruction of event-integrated spectra (spectral fluences) for major solar energetic particle events. *Astronomy and Astrophysics*, *647*, A132. https://doi.org/10.1051/0004-6361/202040058

Korte, M., Mandea, M., & Matzka, J. (2009). A historical declination curve for Munich from different data sources. *Physics of the Earth and Planetary Interiors*, *177*(3–4), 161–172. https://doi.org/10.1016/J.PEPI.2009.08.005

Kovaltsov, G. A., Mishev, A., & Usoskin, I. G. (2012). A new model of cosmogenic production of radiocarbon ^{14}C in the atmosphere. *Earth and Planetary Science Letters*, *337*, 114–120. https://doi.org/10.1016/j.epsl.2012.05.036

Kovalyov, M. (2019). On the correlation of seismic activity to syzygies. *Russian Journal of Earth Sciences*, *19*(1), ES1005–10. https://doi.org/10.2205/2019ES000650

Kromer, B., Manning, S. W., Kuniholm, P. I., Newton, M. W., Spurk, M., & Levin, I. (2001). Regional $^{14}CO_2$ offsets in the troposphere: Magnitude, mechanisms, and consequences. *Science*, *294*(5551), 2529–2532. https://doi.org/10.1126/science.1066114

Kudsk, S. G., Knudsen, M. F., Karoff, C., Baittinger, C., Misios, S., & Olsen, J. (2022). Solar variability between 650 CE and 1900 - Novel insights from a global compilation of new and existing high-resolution ^{14}C records. *Quaternary Science Reviews*, *292*, 107617. https://doi.org/10.1016/J.QUASCIREV.2022.107617

Liang, Q., Douglass, A. R., Duncan, B. N., Stolarski, R. S., & Witte, J. C. (2009). The governing processes and timescales of stratosphere-to-troposphere transport and its contribution to ozone in the Arctic troposphere. *Atmospheric Chemistry and Physics*, *9*(9), 3011–3025. https://doi.org/10.5194/acp-9-3011-2009

McCormac, F. G., Hogg, A. G., Higham, T. F. G., Lynch-Stieglitz, J., Broecker, W. S., Baillie, M. G. L., et al. (1998). Temporal variation in the interhemispheric ^{14}C offset. *Geophysical Research Letters*, *25*(9), 1321–1324. https://doi.org/10.1029/98GL01065

Miyake, F., Hakozaki, M., Kimura, K., Tokanai, F., Nakamura, T., Takeyama, M., & Moriya, T. (2022). Regional differences in carbon-14 data of the 993 CE cosmic ray event. *Frontiers in Astronomy and Space Sciences*, *9*, 139. https://doi.org/10.3389/FSPAS.2022.886140

Miyake, F., Jull, A. J. T., Panyushkina, I. P., Wacker, L., Salzer, M., Baisan, C. H., et al. (2017). Large ^{14}C excursion in 5480 BC indicates an abnormal sun in the mid-holocene. *Proceedings of the National Academy of Sciences*, *114*(5), 881–884. https://doi.org/10.1073/pnas.1613144114

Miyake, F., Masuda, K., & Nakamura, T. (2013). Another rapid event in the carbon-14 content of tree rings. *Nature Communications*, *4*(1), 1748. https://doi.org/10.1038/ncomms2783

Miyake, F., Nagaya, K., Masuda, K., & Nakamura, T. (2012). A signature of cosmic-ray increase in ad 774-775 from tree rings in Japan. *Nature*, *486*(7402), 240–242. https://doi.org/10.1038/nature11123

Miyake, F., Panyushkina, I. P., Jull, A. J. T., Adolphi, F., Brehm, N., Helama, S., et al. (2021). A single-year cosmic ray event at 5410 BCE registered in ^{14}C of tree rings. *Geophysical Research Letters*, *48*(11). https://doi.org/10.1029/2021GL093419

Nevanlinna, H., & Kataja, E. (1993). An extension of the geomagnetic activity index series aa for two solar cycles (1844–1868). *Geophysical Research Letters*, *20*(23), 2703–2706. https://doi.org/10.1029/93GL03001

Oeschger, H., Siegenthaler, U., Schotterer, U., & Gugelmann, A. (1975). A box diffusion model to study the carbon dioxide exchange in nature. *Tellus*, *27*(2), 168–192. https://doi.org/10.3402/tellusa.v27i2.9900

O'Hare, P., Mekhaldi, F., Adolphi, F., Raisbeck, G., Aldahan, A., Anderberg, E., et al. (2019). Multiradionuclide evidence for an extreme solar proton event around 2,610 B.P. (660 BC). *Proceedings of the National Academy of Sciences*, *116*(13), 5961–5966. https://doi.org/10.1073/pnas.1815725116

Paleari, C., Mekhaldi, F., Adolphi, F., Christl, M., Vockenhuber, C., Gautschi, P., et al. (2022). Cosmogenic radionuclides reveal an extreme solar particle storm near a solar minimum 9125 years BP. *Nature Communications*, *13*(1), 214. https://doi.org/10.1038/s41467-021-27891-4

Park, J., Southon, J., Fahrni, S., Creasman, P. P., & Mewaldt, R. (2017). Relationship between solar activity and Δ^{14}C peaks in AD 775, AD 994, and 660 BC. *Radiocarbon*, *59*(4), 1147–1156. https://doi.org/10.1017/RDC.2017.59

Pearson, C., Wacker, L., Bayliss, A., Brown, D., Salzer, M., Brewer, P., et al. (2020). Annual variation in atmospheric ^{14}C between 1700 BC and 1480 BC. *Radiocarbon*, *62*(4), 1–14. https://doi.org/10.1017/rdc.2020.14

Poluianov, S., Kovaltsov, G. A., Mishev, A. L., & Usoskin, I. G. (2016). Production of cosmogenic isotopes ^{7}Be, ^{10}Be, ^{14}C, ^{22}Na, and ^{36}Cl in the atmosphere: Altitudinal profiles of yield functions. *J. Geophys. Res. (Atm.)*, *121*(13), 8125–8136. https://doi.org/10.1002/2016JD025034

Rao, T. N., & Kirkwood, S. (2005). Characteristics of tropopause folds over Arctic latitudes. *Journal of Geophysical Research: Atmospheres*, *110*(D18), 1–13. https://doi.org/10.1029/2004JD005374

Scifo, A., Kuitems, M., Neocleous, A., Pope, B. J. S., Miles, D., Jansma, E., et al. (2019). Radiocarbon production events and their potential relationship with the Schwabe cycle [Dataset]. Scientific Reports, *9*(1), 1–8. https://doi.org/10.1038/s41598-019-53296-x

Scott, E. M., Naysmith, P., & Cook, G. T. (2018). Why do we need ^{14}C inter-comparisons?: The Glasgow-^{14}C inter-comparison series, a reflection over 30 years. *Quaternary Geochronology*, *43*, 72–82. https://doi.org/10.1016/j.quageo.2017.08.001

Scott, E. M., Naysmith, P., & Dunbar, E. (2023). Preliminary results from Glasgow international radiocarbon intercomparison. *Radiocarbon*, *00*, 1–8. https://doi.org/10.1017/RDC.2023.64

Shapiro, M. A., Hampel, T., & Krueger, A. J. (1987). The Arctic tropopause fold. *Monthly Weather Review*, *115*(2), 444–454. https://doi.org/10.1175/1520-0493(1987)115⟨0444:TATF⟩2.0.CO;2

Sookdeo, A., Kromer, B., Büntgen, U., Friedrich, M., Friedrich, R., Helle, G., et al. (2020). Quality dating: A well-defined protocol implemented at ETH for high-precision ^{14}C-dates tested on late glacial wood. *Radiocarbon*, *62*(4), 891–899. https://doi.org/10.1017/RDC.2019.132

Stenke, A., Schraner, M., Rozanov, E., Egorova, T., Luo, B., & Peter, T. (2013). The SOCOL version 3.0 chemistry-climate model: Description, evaluation, and implications from an advanced transport algorithm. *Geoscientific Model Development*, *6*(5), 1407–1427. https://doi.org/10.5194/gmd-6-1407-2013

Stuiver, M., & Braziunas, T. F. (1998). Anthropogenic and solar components of hemispheric ^{14}C. *Geophysical Research Letters*, *25*(3), 329–332. https://doi.org/10.1029/97GL03694

Stuiver, M., Reimer, P., & Braziunas, T. (1998a). Intcal98 radiocarbon age calibration, 24,000-0 cal bp. *Radiocarbon*, *40*(3), 1127–1151. https://doi.org/10.1017/s0033822200019172

Stuiver, M., Reimer, P. J., & Braziunas, T. F. (1998b). High-precision radiocarbon age calibration for terrestrial and marine samples [Dataset]. Radiocarbon, *40*(3), 1127–1151. https://doi.org/10.1017/S0033822200019172

Takeyama, M., Moriya, T., Saitoh, H., Miyahara, H., Miyake, F., Ohyama, M., et al. (2023). Present status of the YU-AMS system and its operation over the past 10 years. *Nuclear Instruments and Methods in Physics Research Section B: Beam Interactions with Materials and Atoms*, *538*, 30–35. https://doi.org/10.1016/j.nimb.2023.01.021

Tarasick, D. W., Carey-Smith, T. K., Hocking, W. K., Moeini, O., He, H., Liu, J., et al. (2019). Quantifying stratosphere-troposphere transport of ozone using balloon-borne ozonesondes, radar windprofilers and trajectory models. *Atmospheric Environment*, *198*, 496–509. https://doi.org/10.1016/j.atmosenv.2018.10.040

Telegadas, K. (1971). *The seasonal atmospheric distribution and inventories of excess carbon-14 from march 1955 to july 1969 (HASL Rep. No. 243)*. Health and Safety Lab., U.S. At. Energy Comm. (Available as HASL243 (accession code) from Natl. Tech. Inf. Serv., Springfield, Va).

Terrasi, F., Marzaioli, F., Buompane, R., Passariello, I., Porzio, G., Capano, M., et al. (2020). Can the ^{14}C production in 1055 CE be affected by SN1054? *Radiocarbon*, *00*(5), 1–16. https://doi.org/10.1017/rdc.2020.58

Usoskin, I. G. (2023). A history of solar activity over Millennia. *Living Reviews in Solar Physics*, *20*(1), 2. https://doi.org/10.1007/s41116-023-00036-z

Usoskin, I. G., & Kovaltsov, G. A. (2021). Mind the gap: New precise ^{14}C data indicate the nature of extreme solar particle events. *Geophysical Research Letters*, *48*(17), e2021GL094848. https://doi.org/10.1029/2021GL094848

Usoskin, I. G., Kromer, B., Ludlow, F., Beer, J., Friedrich, M., Kovaltsov, G. A., et al. (2013). The AD775 cosmic event revisited: The sun is to blame. *Astronomy and Astrophysics*, *552*, L3. https://doi.org/10.1051/0004-6361/201321080

Uusitalo, J., Arppe, L., Hackman, T., Helama, S., Kovaltsov, G., Mielikäinen, K., et al. (2018). Solar superstorm of AD 774 recorded subannually by Arctic tree rings. *Nature Communications*, *9*(1), 3495. https://doi.org/10.1038/s41467-018-05883-1

Uusitalo, J., Arppe, L., Helama, S., Mizohata, K., Mielikäinen, K., Mäkinen, H., et al. (2022). From lakes to ratios: ^{14}C measurement process of the Finnish tree-ring research consortium. *Nuclear Instruments and Methods in Physics Research Section B: Beam Interactions with Materials and Atoms*, *519*, 37–45. https://doi.org/10.1016/j.nimb.2022.03.013

Uusitalo, J., Golubenko, K., Arppe, L., Brehm, N., Hackman, T., Hayakawa, H., et al. (2024). Transient offset in 14C after the Carrington event recorded by polar tree rings - Supplementary data [Dataset]. Zenodohttps://doi.org/10.5281/zenodo.10706817

Wacker, L., Bonani, G., Friedrich, M., Hajdas, I., Kromer, B., Němec, M., et al. (2010). Micadas: Routine and high-precision radiocarbon dating. *Radiocarbon*, *52*(2), 252–262. https://doi.org/10.1017/S0033822200045288

Zhang, Q., Sharma, U., Dennis, J. A., Scifo, A., Kuitems, M., Büntgen, U., et al. (2022). Modelling cosmic radiation events in the tree-ring radiocarbon record. *Proceedings of the Royal Society A*, *478*(2266), 478. https://doi.org/10.1098/rspa.2022.0497